Mechanistic insights into fast adsorption of perfluoroalkyl substances on carbonate-layered double hydroxides

Yun Chen[1,2,3,4], Anett Georgi[4*], Wenying Zhang[1,2,3], Frank-Dieter Kopinke[4], Jingchun Yan[1,3], Navid Saeidi[4], Jing Li[1,3], Mingyue Gu[5], Mengfang Chen[1,3*]

1. Key Laboratory of Soil Environment and Pollution Remediation, Institute of Soil Science, Chinese Academy of Sciences, Nanjing 210008, China

2. University of Chinese Academy of Sciences, Beijing 100049, China

3. Jiangsu Engineering Laboratory for Soil and Groundwater Remediation of Contaminated Sites, Institute of Soil Science, Chinese Academy of Sciences, Nanjing 210008, China

4. Helmholtz Centre for Environmental Research - UFZ, Department of Environmental Engineering, D-04318 Leipzig, Germany

5. Nanjing Kaiye Environmental Technology Co Ltd, Nanjing University Science Park, Nanjing 210034, China

[*] Corresponding author. E-mail: mfchen@issas.ac.cn (Mengfang Chen)

[*] Corresponding author. E-mail: anett.georgi@ufz.de (Anett Georgi)

Abstract

Layered double hydroxide (LDH) with the metal composition of Cu(II)Mg(II)Fe(III) was prepared as an adsorbent for fast adsorption of perfluorooctane sulfonate (PFOS) and perfluorooctanoate (PFOA). 84% of PFOS and 48% of PFOA in relation to the equilibrium state were adsorbed in the first minutes of contact with 0.1 g/L of suspended µm-sized LDH particles. The adsorption mechanisms of PFOS and PFOA on the CuMgFe-LDH were interpreted. Hydrophobic interactions were primarily responsible for the adsorption of these compounds in accordance with the different adsorption affinities of long-chain (C8, K_d = 10^5 L/kg) and short-chain (C4, K_d = 10^2 L/kg) perfluorinated carboxylic acids. PFOA adsorption on CuMgFe-LDH was strongly suppressed under alkaline conditions while PFOS uptake was only slightly affected in the pH range from 4.3 to 10.7, indicating a significant role of electrostatic interactions for PFOA adsorption. The adsorption of PFOS and PFOA was rather insensitive to competition by monovalent anions. The previously reported 'memory effect' of calcined CuMgFe-LDH for sorption of organic anions was not confirmed in the present study. Spent CuMgFe-LDH could be easily regenerated by extraction with 50 vol.% methanol in water within 1 h and maintained a high PFOS removal in subsequent usage cycles.

Key words: LDHs, PFOS, PFOA, Adsorption kinetics, Adsorbent regeneration

1 Introduction

Perfluoroalkyl substances (PFAS) represent a large group of man-made chemicals used in a variety of consumer products and industrial processes, including firefighting foams, adhesives, paper and fabric protection products and in aerospace industry [1,2]. Many PFAS, such as perfluoroalkyl carboxylic acids (PFCAs) and perfluoroalkyl sulfonates (PFSAs), consist of a hydrophobic alkyl chain with varying length (typically C4-C14) and a hydrophilic head group [3]. They have a high chemical stability because of the high C-F bond energies (around 531.5 kJ/mol), which make them particularly persistent in environmental media [4,5]. PFAS have attracted increasing worldwide concern due to their long-term negative impact on animals and humans such as endocrine-disrupting activity, carcinogenesis, neurotoxicity, and reproductive toxicity etc. [6,7]. Some methods have been developed to remove PFAS from contaminated waters, such as adsorption, photo-oxidation and -reduction and electrochemical oxidation [8–13], among which adsorption was considered to be an effective and technically simple method. Ion exchange resins and activated carbon were the most studied adsorbents due to their high adsorption affinity for PFOS and PFOA. However, PFAS adsorption on these adsorbents is rather slow and strongly inhibited in case of ion exchange resins by a real wastewater matrix containing inorganic anions [8,14,15]. Therefore, it is desirable to develop new adsorbents that overcome these shortcomings, i.e. possessing high adsorption rates and being less sensitive to water matrix components. In addition, non-carbonaceous adsorbents offer a wider spectrum of regeneration options including advanced oxidation processes due their inertness even against strongly oxidizing reagents.

Layered double hydroxides (LDHs), also known as hydrotalcite-like compounds, are anionic clay materials [16]. They consist of brucite-like layers with positive surface charge and an interlayer region with charge-compensating anions [17]. Owing to their properties of positive surface charge and anion exchange capacity, LDHs have been applied to remove polluting anions [18], such as

arsenate [19], chromate [20], radionuclides [21] and anionic surfactants [22]. Recently, LDHs and their calcined products, i.e. layered double oxides (LDOs), were also studied for the removal of PFOS and PFOA from water and a fast adsorption kinetics was observed [9,23]. However, in these studies, PFOS and PFOA were applied with rather high concentrations (C_e = 19-1900 μmol/L). In addition, the variable metal composition of LDHs is one of their unique properties which might have an effect on their adsorptive performance, while only MgAl-LDH was examined to date. Lastly, the reusability of LDHs or LDOs and the reversibility of PFAS adsorption on LDHs or LDOs were not explored.

Therefore, in the present work, LDHs with various metal compositions and an interlayer of CO_3^{2-} as charge-balancing anions were synthesized and employed to adsorb typical PFAS such as PFOA and PFOS with equilibrium aqueous phase concentrations ranging from 0.05 to 1.0 μmol/L. The adsorption behavior of PFOA and PFOS on LDHs as single and mixed solutes under different water chemistry conditions was elucidated. The effects of thermal treatment of LDHs on the adsorption of PFOA and PFOS were studied and the reusability of LDHs was evaluated.

2 Materials and Methods

2.1 Chemicals and material synthesis

Common chemicals used in this work are listed in Table S1. The PFAS including PFOS (≥ 98%), perfluorononanoic acid (PFNA, ≥97%), PFOA (≥97%) and perfluorobutanoic acid (PFBA, ≥98%) were purchased from ALDRICH (Germany). Perfluorobutane sulfonate (PFBS, ≥98%) was bought from ABCR (Germany). Their properties are listed in Table S2. All chemicals were used without further purification.

LDHs were synthesized by the co-precipitation method reported before [24]. The procedure is briefly described as follows: a metal solution with 0.6 mol/L M^{2+} and 0.2 mol/L M^{3+} was prepared

and dropped into a flask containing 50 mL deionized water and maintaining pH at 10.0 ± 0.3 controlled by a pH automatic titrator. Intense stirring was employed during the whole dropping process. The obtained suspensions were aged for 22 h and then washed with deionized water and ethanol. Finally, the obtained solid was dried overnight at 100^{o}C.

2.2 Adsorbents characterization and PFAS analysis

The prepared materials were structurally characterized using X-ray diffraction (XRD) on a diffractometer with Cu Kα radiation (Ultima IV). Fourier transform infrared spectra (FTIR, Nicolet iS10 Thermo Scientific spectrometers, 1 wt-% in KBr wafers) were measured to determine the surface functional groups of the adsorbents. After and before adsorption of PFAS, the adsorbents were characterized by XRD and FTIR. The loaded samples were prepared as follows: the adsorbents were collected by centrifugation after PFOS and PFOA adsorption for 6 h and dried at 80°C. Then they were divided into two parts, one was pressed with potassium bromide to a thin disk for FTIR characterization. XRD was carried out with the second part directly.

The BELSORP-miniII instrument (Bel, Japan) was used to determine the specific surface area (SSA) and relevant pore size information of adsorbents with the N_2 adsorption/desorption method at -196°C. SSA, pore volume and mean diameter were calculated by an analysis software of BELSORP-miniII with the Brunauer-Emmett-Teller method (BET).

The PFAS concentrations in the liquid phase were determined by liquid chromatography-mass spectrometry (single-stage quadrupole with electrospray ionization, LCMS-2020; SHIMADZU Corporation). The type of column was 100 mm × 2 mm Gemini C6-phenyl filled with fully porous organo-silica having 110 Å pore size and 3 µm particle size (Phenomenex Company). Aliquots of 5 µL for the mixture or 3 µL for the single component experiments were injected onto the column by the autosampler. The mobile phases were a combination of solvent A composed by 10%

methanol and 90% water with 20 mmol/L ammonium acetate and solvent B consisting of 90% methanol and 10% water with 20 mmol/L ammonium acetate. The solvents A and B were delivered at a ratio 3:7 with a flow rate of 0.3 mL/min. The column temperature was maintained at 40^{o}C. The total run times were 10 and 20 min for single and mixed cases, respectively. For concentrations less than 1 mg/L the correlation coefficients (R^2) of the calibration curves for the PFAS were greater than 0.99. The limit of quantification (LOQ) of the PFAS was 0.1 µg/L and the standard deviation for 5 measurements was around 5%. Aqueous samples from batch experiments with high ionic strength (e.g. ≥ 100 mM $NaNO_3$) were diluted by at least a factor of 10 prior to the injection into the LC-MS instrument.

2.3 Adsorption experiments

Adsorption kinetics experiments were conducted in 125 mL glass vessels with screw caps and PTFE-lined septa containing 100 mL solution at room temperature ((23 ± 2) ^{o}C) with 150 rpm shaking. The initial concentrations of each component of PFAS (PFOS and PFOA) were 1.9 µmol/L and the dosage of LDHs was 0.1 g/L. Samples were collected at specific time intervals from 0 to 12 h and rapidly separated in supernatant and sediment by centrifugation. Samples with adsorption time less than 5 min were filtered using syringe filters (0.2 µm regenerated cellulose membrane) which showed negligible PFAS adsorption during the fast filtration step.

Isotherm experiments were carried out in 7.0 mL vessels containing 5.0 mL solution and sacrificial sampling was employed. The initial concentrations of each component of PFOS and PFOA were changed from 0.093 µmol/L to 1.86 µmol/L in order to achieve adsorption isotherms. The pH value was adjusted to 7.0 in the above experiments. 1.0 mol/L HNO_3, NaOH and $NaNO_3$ were used to adjust initial pH from 3.0 to 11.0 and ionic strength from 3 to 200 mmol/L during the investigation of the impact of ionic strength and pH values on the adsorption of PFOS and PFOA. In addition, NaCl and Na_2SO_4 were employed to study the influence of inorganic anions.

In order to assess the reversibility of the PFOS and PFOA adsorption process, 2.0 mL methanol or acetonitrile were added to 2.0 mL aqueous suspensions containing 0.1 g/L LDH following the equilibrium of PFOS and PFOA adsorption. The vials were shaken for 1 to 6 h. During the experiments on the regeneration and reusability of LDHs, the suspensions were separated by centrifugation and then a mixture of 5.0 mL solvent containing 50 vol% methanol and 50 vol% deionized water was added into the vial. After shaking for 24 h, the LDH particles were separated and washed with deionized water. The collected LDHs were dried in an oven at 100^{o}C and reused in the next adsorption cycle.

The aqueous supernatant was separated for PFAS analysis (by LC-MS) by centrifugation. All experiments were carried out in duplicate and a parallel control without adsorbents was also set up as a reference for the initial concentration before adsorption (C_0). The recovery of PFAS in these parallel controls was within (100 ± 6) %, indicating limited loss of PFAS on glass vessels in our study.

The amount of PFOS and PFOA adsorbed by the adsorbents and the single-point adsorption coefficients K_d (L/g) were calculated from eq. (1) and (2)

$$q_t = (C_0 - C_t)/C_s \quad (1)$$

$$K_d = q_e/C_e \quad (2)$$

where q_t and q_e (μmol/g) are the concentrations of adsorbed solutes on the adsorbents at time t (min) and at equilibrium, respectively. C_0 (μmol/L) is the initial solute concentration. C_t and C_e (μmol/L) are solute concentrations in the aqueous phase at time t and at equilibrium, respectively. C_s (g/L) is the dosage of the adsorbents.

3 Results and Discussion

3.1 Sorption kinetics and isotherms

3.1.1 PFOS and PFOA sorption kinetics

Fig. S1 presents the results of PFOA and PFOS removal by six LDHs-CO_3^{2-}, namely CuMgFe-LDH, CuMgAl-LDH, CuNiFe-LDH, MgFe-LDH, MgAl-LDH and ZnAl-LDH. Considering the removal efficiencies of PFOA and PFOS and the environmental compatibility of the metal compositions in various LDHs, CuMgFe-LDH was selected to study the adsorption behavior of PFOA and PFOS in the following experiments in more detail. The data of adsorption kinetics on the CuMgFe-LDH are presented in Fig. 1, which suggests that significant adsorption took place in the initial first minutes and the adsorption equilibria were all approached within 1-3 h. This is considered to be fast compared to the typical equilibration time ranges reported for ion exchange resin materials (2-168 h), granular carbon (4-240 h) and most powder carbon materials (1-24 h) [25].

CuMgFe-LDH possesses a higher PFOS adsorption than PFOA under both single and mixed adsorption scenarios (Fig. 1), which is in conformity with previous studies [26]. This difference is mainly caused by the higher hydrophobicity of PFOS having one more CF_2 unit compared to PFOA. This view is supported by the much lower difference in K_d values of PFNA and PFOS (Fig. 4a and related discussion in section 3.2.2), both having the same number of CF_2 groups. This finding suggests that there is not a strong difference regarding the effects of the carboxylic or sulfonate head groups on the adsorption to the LDH materials. Moreover, uptake of PFOS and PFOA was not significantly impacted by their co-existence in mixed adsorption experiments in case of low total PFAS loadings (<1.3 wt.%). Possible competition effects are considered in more detail in Section 3.1.2.

Generally, the adsorption of an adsorbate from liquid phase to an adsorbent surface is considered as a three-step process: (i) diffusion across a stagnant liquid film surrounding the adsorbent particle (film diffusion or external mass transfer); (ii) diffusion inside the adsorbent particle (intraparticle diffusion or internal mass transfer) and (iii) adsorption on the pore surface of the adsorbent (surface reaction) [27]. However, common kinetic models, such as pseudo-first-order or pseudo-second-order models are based on the assumption that the overall rate of adsorption is controlled by the surface reaction while they neglect the two diffusion steps which may be also significant for many adsorption processes [28].

The pseudo-second order model is often used to describe adsorption kinetics of PFAS to activated carbon materials. However, the obtained pseudo-second order rate coefficients (k_2) strongly depend on the applied conditions (e.g. adsorbent dosage). This leads to a high variation in k_2 for PFAS adsorption to powder AC samples (ranging from 0.01 to 100 g/mg/h) determined in various studies under different conditions [25]. The pseudo-second order model fits PFOA and PFOS adsorption kinetics to the LDH material better than the first-order kinetics model. The resulting rate constants are 3.9 and 5.4 g/mg/h, respectively (Fig. S2). However, considering the above-mentioned shortcomings of this model, it is focused on the determination of surface diffusion coefficients as an intrinsic material-based property. Film mass transfer (k_f) and surface diffusion coefficients (D_s) were determined in this study using a simplified method suggested by Yao and Chen (2015) and further described in the SI part. These step-based kinetic parameters are more suitable for the prediction of kinetics under various adsorption scenarios and are used to discuss the adsorption processes of PFOS and PFOA on CuMgFe-LDH. Based on the simplified method, the parameters for calculating k_f and D_s are provided in Table S4. It results that k_f is in the range of $(5.0 \pm 2.5) \times 10^{-5}$ m/s for PFOS and PFOA. This is within the typical range for well mixed particle suspensions under batch conditions. For the surface diffusion coefficient values of $D_s = 2 \times 10^{-18}$ m^2/s for PFOS

198 and $D_s = 3 \times 10^{-17}$ m^2/s for PFOA were determined from mixed solutes experiments. D_s values in
199 the range from 2×10^{-14} to 8×10^{-12} m^2/s were reported by Yao and Chen (2015) for adsorbates of
200 various molecular sizes (from toluene to ampicilline) on different adsorbents including activated
201 carbon, zeolites and organobentonite. The comparatively low intraparticle diffusivity of the PFAS
202 anions in LDHs (10^{-17}-10^{-18} m^2/s) points to strong adsorptive interactions lowering the adsorbate's
203 intraparticle mobility. D_s values were also estimated (which are rarely directly reported) from
204 adsorption kinetics data available in the literature for PFOA and PFOS on other types of adsorbents
205 such as AC, alumina or boehmite (Table 1). Obviously, surface diffusion coefficients of the PFAS
206 anions under these cases are comparatively low, i.e. in a range from 8×10^{-18} to 6×10^{-16} m^2/s.
207 This slow intra-particle diffusion must be compensated for by small particle sizes, in order to keep
208 the adsorption times manageable. This requirement is stressed by the fact that intraparticle diffusion
209 rates are proportional to the square of adsorbent particle size (eq 2. in SI). The µm-sized LDH
210 particles (d_{50} = 3 µm, Fig. S3) are providing beneficiary adsorption rates. They are obtainable by a
211 simple bottom-up process and don't require energy-intensive milling of larger particles. On the
212 other hand, this particle size can be still separated by sedimentation or micro-filtration from treated
213 waters.
214

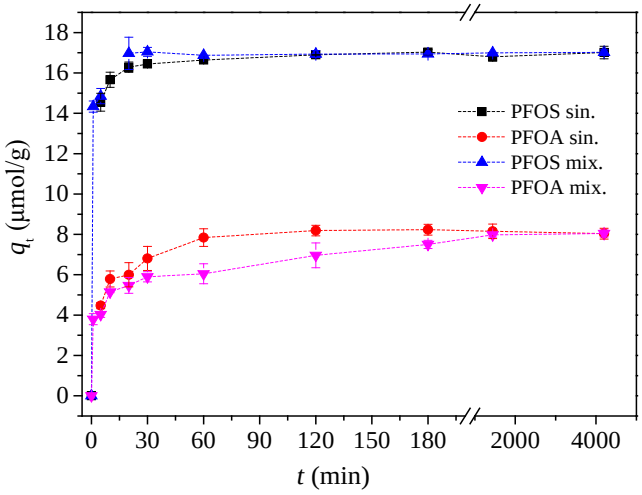

Fig. 1. Kinetics of the adsorption of PFOS and PFOA on CuMgFe-LDH under single and mixed solutes conditions. Note: PFOS sin. and PFOA sin. represent single solute adsorption; PFOS mix. and PFOA mix. represent mixtures of PFOS and PFOA; experimental conditions: C_0 = 1.9 μmol/L for PFOS or PFOA, adsorbent dosage of 0.1 g/L, pH = 7.0. Error bars are deviations of single values from the mean of two experiments.

Table 1 Comparison of surface diffusion coefficients in adsorption of PFAS to LDHs and other adsorbent materials

Adsorbent	Adsorbate	Size (mm)	Mean pore size (nm)	D_s (m^2/s)	Reference
Activated carbon fiber	PFOS	0.01	2.4	1.7×10^{-17}	[29]
Activated carbon fiber	PFOA	0.01	2.4	2.1×10^{-17}	[29]
Powder activated carbon	PFOS	0.005	2.1	8.2×10^{-18}	[29]
Powder activated carbon	PFOA	0.005	2.1	1.5×10^{-17}	[29]
Alumina	PFOS	0.08	-	1.1×10^{-16}	[30]
Alumina	PFOA	0.08	-	6.3×10^{-16}	[30]
Boehmite	PFOS	0.037	-	1.1×10^{-17}	[26]
Boehmite	PFOA	0.037	-	9.6×10^{-17}	[26]
CuMgFe-LDH	PFOS	0.003	41	2.0×10^{-18}	This work
CuMgFe-LDH	PFOA	0.003	41	3.3×10^{-17}	This work

3.1.2 PFOS and PFOA adsorption isotherms

Adsorption isotherm experiments were performed with PFOS and PFOA separately, and a mixture of both at pH = 7.0 At this pH the net surface charge of the adsorbents is positive (pH_{pzc} = 7.9) and both PFOS and PFOA are anions. Amphiphilic compounds may be adsorbed onto the external surface of minerals in hemi-micelles when the organic ions are present at two or three orders of magnitudes less than the critical micelle concentrations in solution [26] which is around 8 mmol/L and 25 mmol/L [31] for PFOS and PFOA, respectively. In the present study, the maximum initial concentration of the adsorbates was 1.9 μmol/L and thus in a range where hemi-micelle formation at the external surface is considered less likely. The Freundlich isotherm model, a commonly used adsorption model, was used to fit the experimental data. The model is expressed as eq. (3):

$$q_e = K_F \times C_e^n \qquad (3)$$

where q_e in μmol/g is the equilibrium concentration (loading) of adsorbed solute on adsorbent. C_e in μmol/L is the concentration of solute in the aqueous phase at equilibrium. K_F (μmol/g)/(μmol/L)^n is the Freundlich constant that indicates the affinities between adsorbents and adsorbates; n (dimensionless) is the Freundlich exponent related to the non-linearity of the isotherm. The determined fitting parameters were listed in Table 1. As shown in Fig. 2, the isotherms could be well fitted by the Freundlich model with correlation coefficients (R^2) being larger than 0.91 regardless of the presence of single compounds PFOS or PFOA or their mixture. The corresponding linearized fitting of the isotherms is presented in Fig. S4. Other isotherm models, such as Langmuir and Virial models, failed to fit the data. Freundlich exponents $n > 1$ (Table 2) suggest beneficial interactions between adsorbate molecules rather than surface competition. It was tested whether this benefit is also obtained by the mixed adsorbate molecules of PFOS and PFOA. The non-linearity of the isotherm increased for PFOS (n became larger, Table 1 and red curve above black curve in Fig. 2 b) meaning that PFOS could take profit from the concurrent adsorption of PFOA

especially in the higher loading range. On the other hand, changes for PFOA are less pronounced. The assumption that the less adsorbed PFOA could significantly benefit from adsorbate interactions with PFOS cannot be confirmed. The same holds for other shorter-chain perfluorocarboxylic acids as shown in section 3.2.2.

In order to compare CuMgFe-LDH with other adsorbents, K_d values at a certain equilibrium aqueous phase concentration (C_e) of PFOS or PFOA were calculated from isotherm plots and Freundlich isotherm parameters reported in the literature (Table S5). The LDH material ranks well among several AC, biochar and polymer materials in PFOS adsorption with K_d in the range of (0.27-1.0) × 10^5 L/kg at C_e = 25-80 µg/L. However, it does not reach the range of K_d of high-performance AC adsorbents (>10^6 L/kg). Nevertheless, possible advantages of the LDH material over AC materials result from the fact that it is a mineral adsorbent which is resistant towards strong oxidants and thus could be combined with sulfate radical-driven oxidation processes for PFAS degradation [32] and can be synthesized in µm-particle size by a facile bottom-up approach.

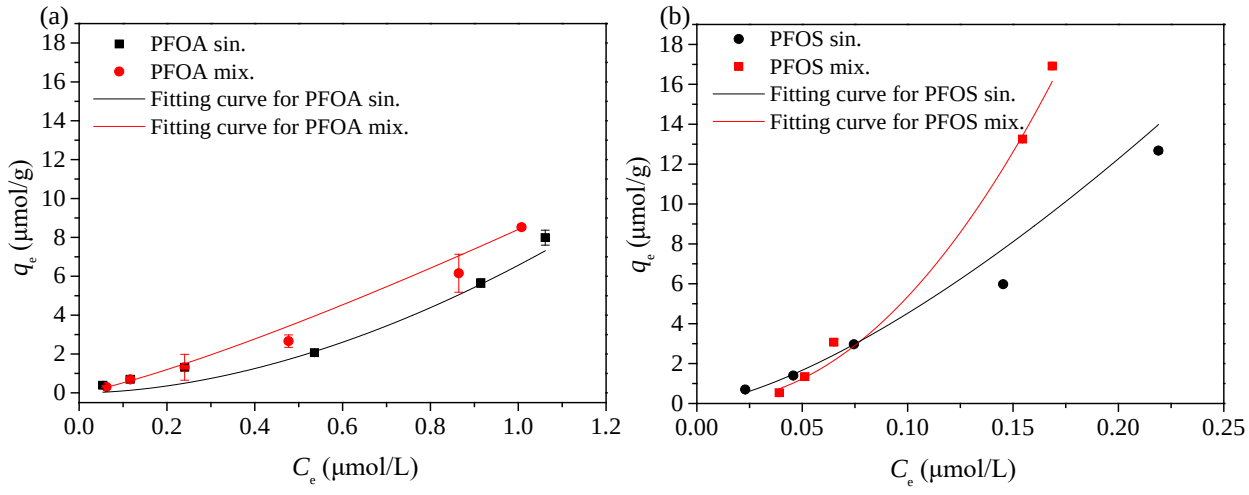

Fig. 2. Adsorption isotherms of PFOA and PFOS on CuMgFe-LDH with (a) single and (b) mixed adsorbates. Experimental conditions: C_0 = 0.093 to 1.86 µmol/L PFOS or PFOA, adsorbent dosage

of 0.1 g/L, pH = 7.0 and adsorption time of 6 h. Error bars were deviations of single values from the mean of two experiments.

Table 2. Fitting parameters of Freundlich isotherms for adsorption of PFOA and PFOS on CuMgFe-LDH

Solutes	n	K_F (μmol/g)/(μmol/L)^n	R^2
PFOS sin.	1.4	124	0.99
PFOS mix	2.1	694	0.99
PFOA sin.	1.8	6.5	0.91
PFOA mix	1.2	8.4	0.99

3.2 Adsorption mechanism

As it was stated in previous studies, the adsorption behavior of PFOS or PFOA can be driven by various forces including surface electrostatic attraction, hydrophobic interaction, H-bond effect and interlayer anion exchange on various adsorbents [3,25]. The exchange between NO_3^- and PFOS anions in MgAl-LDH with NO_3^- as interlayer anions and the intercalation of PFOA due to a restructuring effect of calcined MgAl-LDH were reported to be predominated under high PFOS and PFOA concentrations (C_e = 18.6-1860 μmol/L) [9,23]. In this study, the adsorption mechanism at low concentrations (C_e = 0.05-1.0 μmol/L) of PFOS and PFOA on CuMgFe-LDH with carbonate as interlayered anion were explored.

3.2.1 The role of electrostatic attraction

As pH and ionic strength of the medium affect the surface charge of adsorbents, PFOS and PFOA adsorption would be strongly influenced by a change in these parameters if electrostatic attraction was the main driving force. The net surface charge of CuMgFe-LDH was changed from positive to negative when the solution approaches pH > 7.9 according to the point of zero charge of CuMgFe-LDH. Generally, in case of the positively charged surface, electrostatic attraction of

anions would be weakened at high ionic strength due to the double layer compression effect [33]. As illustrated in Fig. 3a, the loading of PFOS and PFOA was decreased by a factor of 1.3 and 2.2 respectively at pH 7.0 with $NaNO_3$ concentrations being increased from 0 to 100 mmol/L. No significant difference was observed between single and mixed PFOS and PFOA adsorption batch experiments. The single point adsorption coefficients K_d of PFOA and PFOS on the LDH were also calculated to show the changes of adsorption affinities under various $NaNO_3$ concentrations (Fig. S6a). With the concentrations of $NaNO_3$ being increased from 0 to 100 mmol/L at pH 7.0, log (K_d/(L/kg)) of PFOS and PFOA decreased from 4.97 and 3.97 to 4.35 and 3.23, respectively, indicating a significant decrease of adsorption affinities when weakening electrostatic attraction. In contrast, PFOA adsorption was improved at high ionic strength (Fig. 3b) at pH 10.7 since the electrostatic repulsion of the carboxylate group by the negatively charged surface of CuMgFe-LDH was suppressed.

In addition to $NaNO_3$, also NaCl and Na_2SO_4 were used as electrolytes to study the impact of competitive anions on the adsorption of PFOS and PFOA. Because of the similar changes of PFOS and PFOA adsorption upon changes in ionic strength under the single or mixed solute scenarios, the subsequent experiments were only undertaken for the mixture of PFOS and PFOA. As illustrated in Fig. S7, adsorption affinities of PFOS and PFOA on CuMgFe-LDH are slightly decreased in the presence of 10 mmol/L NaCl or $NaNO_3$. This effect is much stronger with 10 mmol/L of Na_2SO_4, with a decline in log (K_d/L/kg) by 1.1 and 1.5 units for PFOS and PFOA, respectively. Additionally, the ionic strength of 1 mmol/L Na_2SO_4 is equal to that of 3 mmol/L $NaNO_3$ solution, but the log (K_d/L/kg) of PFOS and PFOA in 1 mmol/L Na_2SO_4 was 4.0 and 2.5 (Fig. S7) while it was 4.8 and 3.7 in 3 mmol/L $NaNO_3$ (Fig. S6), respectively, which means that SO_4^{2-} has a more negative effect on PFOS and PFOA adsorption than NO_3^- at the same ionic strength. The results are in accordance with previous findings that the divalent SO_4^{2-} anion has a

311 higher affinity to the LDH surface than monovalent anions such as Cl^- and NO_3^- [34]. In addition,
312 the negative effect of co-existing anions was stronger for PFOA than PFOS irrespective of the
313 applied anions, suggesting that the electrostatic attraction is more significant for PFOA compared
314 with PFOS adsorption.
315 Similar results were also obtained for the effect of the pH value on the adsorption of PFOS and
316 PFOA. The negative surface charge of CuMgFe-LDH at pH = 10.7 decreased the adsorption of
317 PFOS or PFOA anions. As presented in Fig. 3b, PFOS adsorption was only slightly declined from
318 16.8 to 14.1 μmol/g while only 0.9 μmol/g PFOA was remained adsorbed when the pH values were
319 increased from 7.0 to 10.7, which indicated that electrostatic interactions play a more important
320 role in PFOA than PFOS adsorption. Previous studies [35] reported that PFOS or PFOA uptake
321 would rise with a decrease in pH due to the increase in positive surface charge of the adsorbents.
322 However, q_e decreased slightly in the present study at the lowest tested pH of 4.3. This could be
323 due to the instability of the LDH adsorbents under acidic conditions. Thus, a circum-neutral pH is
324 thought to be optimal for this adsorbent.
325 It is worth noting that the pH sensitivity of the adsorption is less pronounced at high electrolyte
326 concentration of 100 mmol/L. As presented in Fig. 3b, q_e of PFOS and PFOA were maintained at
327 around (11 ± 1) μmol/g and (2.5 ± 0.5) μmol/g, respectively, over the whole pH range from 4.7 to
328 10.7. This trend was in conformity with a previous study [33] as electrostatic interactions (attractive
329 and repulsive) are significantly suppressed due to electrical double layer compression at high ionic
330 strength.

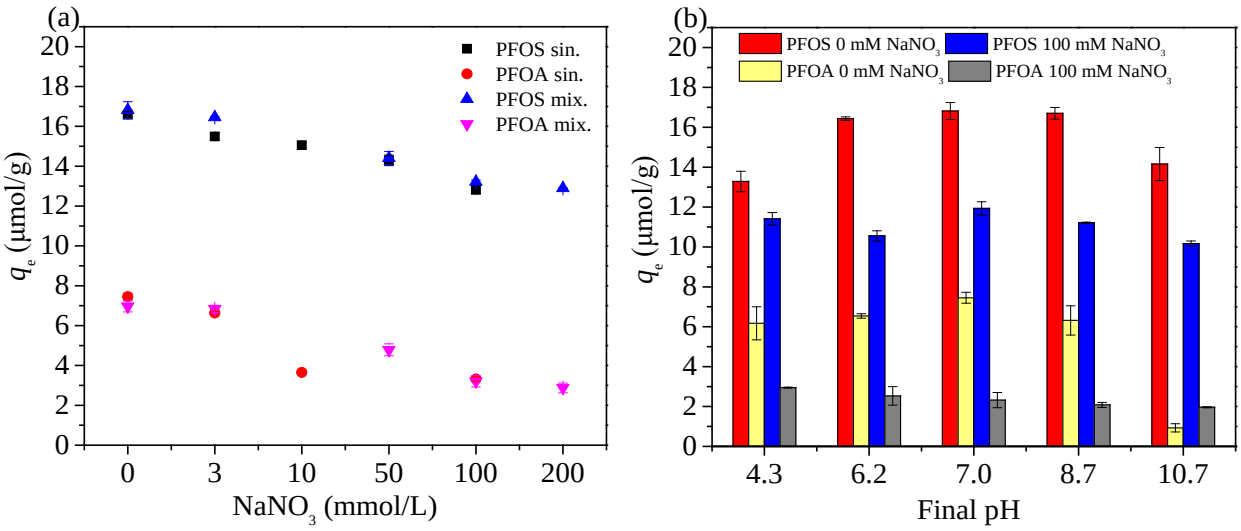

331

332

333 Fig. 3. Loadings of PFOA and PFOS on CuMgFe-LDH under different water matrix conditions:
334 (a) varying $NaNO_3$ concentrations and (b) pH values in case of the mixed solutes. Experimental
335 conditions: C_0 = 1.9 μmol/L PFOS or PFOA, adsorbent dosage of 0.1g/L, pH = 7.0 in Fig. 3a;
336 adsorption time of 6 h. Error bars are deviations of single values from the mean of two experiments.

337

338 **3.2.2 The role of hydrophobic interactions**

339 It was reported that the hydrophobic effect, determined by the length of the perfluorocarbon chain
340 $CF_3(CF_2)_m$, is an important driving force for the adsorption of PFAS and with the increase in *m*,
341 the hydrophobicity of PFAS would also be increased [36]. In the present work, PFNA, PFBA and
342 PFBS were used in addition to PFOA and PFOS in order to evaluate the hydrophobic effects on
343 the adsorption of PFAS. In order to compare the adsorption affinities of PFAS on the CuMgFe-
344 LDH with different number (*m*) of CF_2 units, single point adsorption coefficients (K_d) were
345 calculated and presented in Fig. 4. The decreasing order of adsorption affinities of these PFAS on
346 CuMgFe-LDH was PFOS > PFNA > PFOA >> PFBS > PFBA regardless of their presence as single
347 or mixed components in the solution. It can be concluded that PFBA or PFBS with their short

perfluorocarbon chains (m = 2 or 3) were hardly adsorbed by CuMgFe-LDH with $K_d = 1 \times 10^2$ and 2×10^2 L/kg, respectively. PFOS with the sulfonate head group was a factor of 1.6 better adsorbed on the CuMgFe-LDH ($K_d = 1.1 \times 10^5$ L/kg) than PFNA ($K_d = 6.7 \times 10^4$ L/kg), both adsorbates having the same number of CF_2 units [37]. Within the homologous series of perfluorocarboxylic acids the effect of the chain lengths is very significant: K_d declines by two to three orders of magnitude from PFNA to PFBA (Fig. 4). In summary, we conclude that hydrophobic interaction is the main driving force responsible for the adsorption of PFAS on the studied CuMgFe-LDH under circumneutral pH conditions.

In the case of the bisolute adsorption systems, negligible competitive effects of co-existing PFOS on PFOA and PFNA were noted under the initial concentrations of 1.9 μmol/L and 0.1 g/L of each adsorbate and adsorbent, respectively. PFBA and PFBS were only slightly adsorbed under the applied conditions. Nevertheless, it becomes clear that these shorter-chain acids do not benefit from the concurrent adsorption of PFOS as there was no obvious increase in K_d. Generally, PFOS and PFOA concentrations are very low in common contaminated surface or groundwaters, i.e. in the ng/L to lower μg/L range [5,38]. Thus competitive effects in their adsorption can be ignored in the reality.

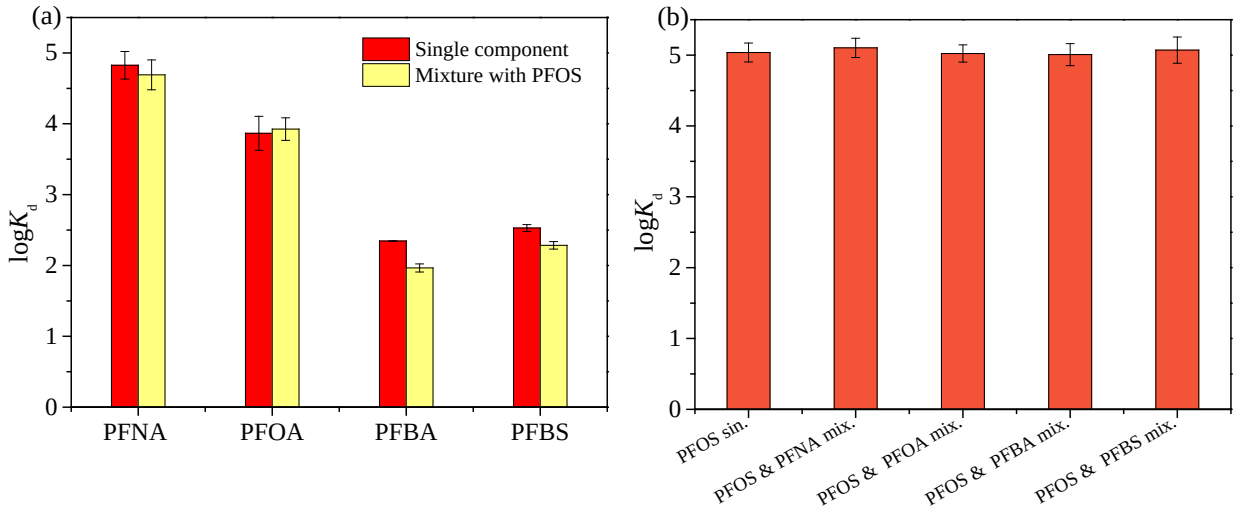

Fig. 4. Single point adsorption coefficients log (K_d /(L/kg)) for (a) PFNA, PFOA, PFBA and PFBS applied as single components as well as mixtures with PFOS and (b) PFOS as single component and in a mixture with the above listed PFAS. Experimental conditions: C_0 = 1.9 μmol/L for PFOS, PFOA, PFNA, PFBS or PFBA, adsorbent dosage of 0.1 g/L, pH = 7.0; adsorption time of 6 h. Error bars show deviations of single values from the mean of two experiments.

3.2.3 The role of anion exchange

According to previous studies interlayer exchange of PFOS and PFOA anions replacing carbonate counterions at LDH increases the basal spacing (d_{003}) of LDH because of the larger size of the PFAS compared to carbonate. In addition, the signal of CO_3^{2-} in the FTIR pattern would be also weakened [23]. As presented by the FTIR pattern in Fig. 5b, new absorption signals at 1205 and 1243 cm^{-1} appeared after PFOS and PFOA adsorption, which can be attributed to vibrations of CF_2 and CF_3 groups, respectively, and directly indicate the adsorption of PFOS and PFOA on CuMgFe-LDH. However, the intensity of the asymmetric stretching of the CO_3^{2-} at around 1362 cm^{-1} almost remained unchanged before and after PFOS and PFOA adsorption. The same is true for the broad absorption bands of the metal-OH stretching and H_2O bound to interlayer anions by H-bonds at 3600-3300 cm^{-1}. In addition to the negligible effect on the surface groups, there was also no

significant change in the interlayer space of CuMgFe-LDH before and after PFAS adsorption (Table S6) in the studied concentration range. As a compensating anion, the loading of carbonate is equal to half of the molar amount of Fe(III) and was estimated to be 1.4 mmol/g which is much higher than the obtained PFAS loading. Therefore, these findings indicate that the extent of ion exchange was too little to show the change in XRD or FTIR spectra. It was reported that CO_3^{2-} exchange with dodecyl sulfates is only significant at high concentrations of 0.3-0.4 mmol/L [39]. In addition, CO_3^{2-} is the hardest interlayer anion to be exchanged attributed to its stability in binding with LDHs[40] Thus, anion exchange is unlikely to occur as a relevant driving force for PFAS adsorption on the studied LDH which is also in agreement with the large difference in adsorption of PFAS with various chain lengths.

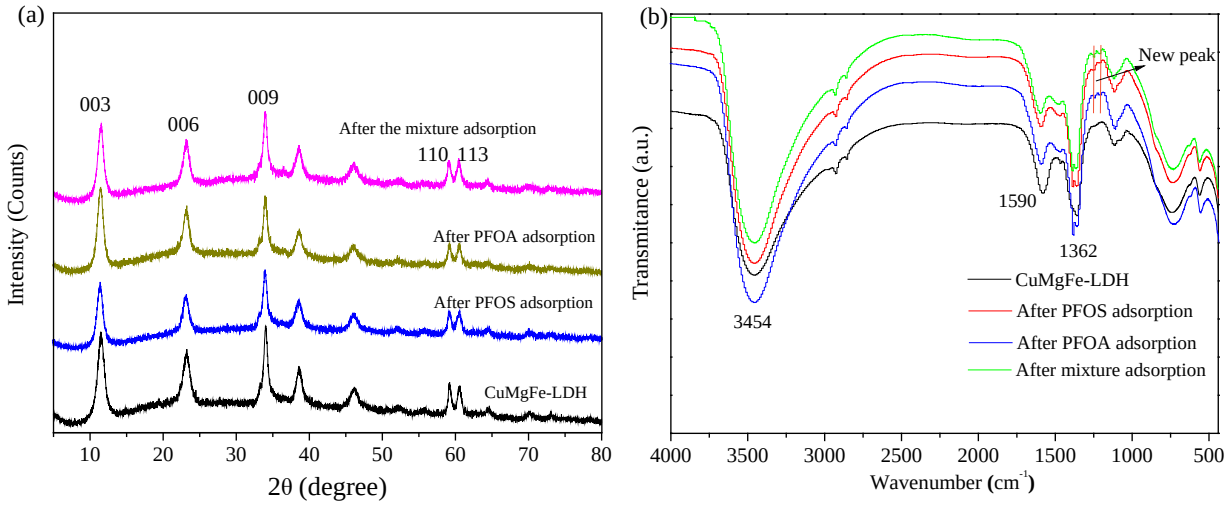

Fig. 5. (a) XRD and (b) FTIR pattern of fresh and PFAS-loaded CuMgFe-LDH. Note: PFOS and PFOA loadings were about 17 and 7 μmol/g, respectively.

3.3 Influence of LDH thermal treatment on PFOS and PFOA adsorption

It was hypothesized that the calcined carbonate LDHs (LDOs) have the ability to adsorb anionic pollutants from aqueous solution dominated by the so called “memory effect”, that means the LDOs could reconstruct part of their original layer structure with rehydration and sorption of

various anions [9]. Therefore, different calcination temperatures were adopted to study the adsorption of PFOS and PFOA on CuMgFe-LDO in the present study. The change of CuMgFe-LDH at different temperatures is described in chapter S2. As shown in Fig. 6a, uptakes of both PFOS and PFOA were decreased if CuMgFe-LDH was calcined compared to the non-calcined cases. The equilibrium loading of PFOA was strongly declined from 7.3 to 0.9 μmol/g on CuMgFe-LDO (300℃) and then kept constant on CuMgFe-LDO (500℃ and 700℃). The loading of PFOS was firstly decreased from 17.1 to 8.5 μmol/g on CuMgFe-LDO (300℃), further to 3.6 μmol/g on CuMgFe-LDO (500℃), then remained unchanged on CuMgFe-LDO (700℃). The low adsorption of PFOA and PFOS on CuMgFe-LDO (700℃) is explained by the huge decline in specific surface areas and pore sizes caused by high temperature calcination. CuMgFe-LDO (300℃ and 500℃) raised suspension pH to about 10.0 after immersion into water. Thus, PFOA and PFOS under low initial concentrations are unlikely to be removed by the "memory effect" of LDO under these alkaline conditions due to the large amount of OH^- competing for uptake into the interlayer. In addition, it was reported that specific interactions between the sulfonate group of PFOS and surface Al-OH also play a role in PFOS adsorption on clay minerals [41]. It is reasonable to speculate that the elimination of the large amount of layered surface OH-groups might be responsible for the further decline of PFOS adsorption on CuMgFe-LDO (500℃) compared to CuMgFe-LDO (300℃) even though their specific surface areas and pore sizes were similar (Table S7). Overall, the calcined CuMgFe-LDOs show a poor performance on PFOS and PFOA adsorption in this study.

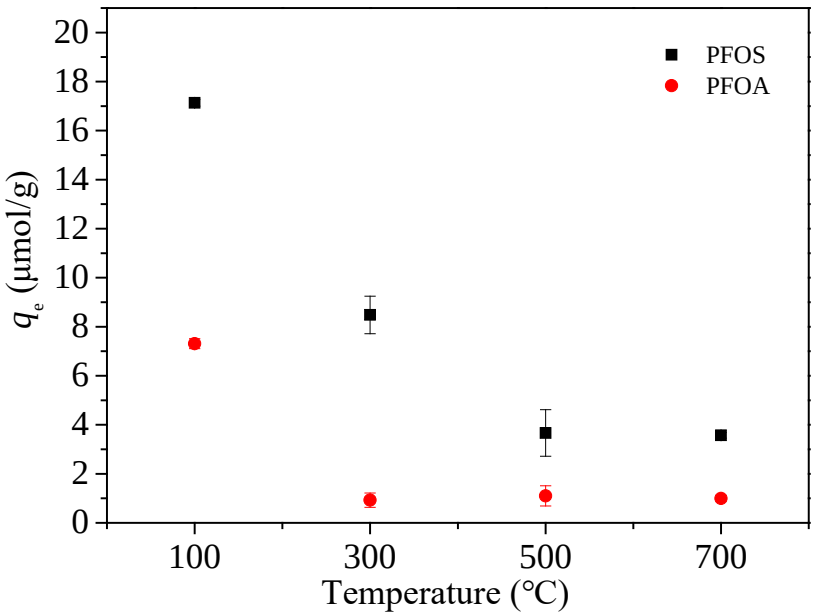

Fig. 6. The impact of CuMgFe-LDH calcination temperature on the adsorption of PFOS and PFOA as mixed solutes. Experimental conditions: C_0 = 1.9 μmol/L for PFOS or PFOA, adsorbent dosage of 0.1 g/L, pH_0 = 7.0 and adsorption time of 6 h. Error bars show deviations of single values from the mean of two experiments.

3.4 Reversibility of PFOS and PFOA adsorption, regeneration and reuse of LDHs

The reversibility of the PFOS and PFOA adsorption was tested by adding 2.0 mL methanol or acetonitrile to 2.0 mL aqueous suspensions with 0.1 g/L CuMgFe-LDH after adsorption of the PFAS. The result is presented in Fig. 7a. PFOS and PFOA were fully desorbed by methanol or acetonitrile addition within 1 h, which suggested that the sorption process of PFOS and PFOA is reversible and covalent bonds were not formed between PFOS (PFOA) and CuMgFe-LDH. A typical regeneration test was accomplished by addition of 5.0 mL (methanol/water = 1:1) to the separated adsorbent (10 mg). The regeneration efficiencies of the spent CuMgFe-LDH and the removal efficiencies of PFOS and PFOA by reused CuMgFe-LDH in three cycles is shown in Fig.7b. The removal of PFOS dropped from 92% in the first run to 82% and 85%, respectively, in the second and third runs. This indicates that the regenerated LDH maintained a steady and high

434 removal efficiency for PFOS in three cycles. Regeneration by simple solvent extraction is worth to
435 be studied in more subsequent steps.

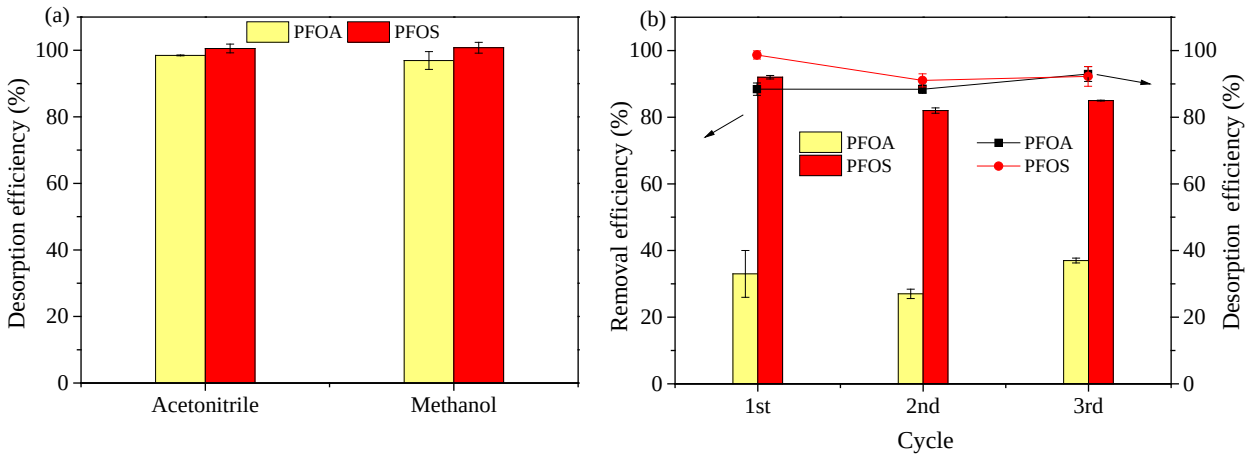

436

437 Fig. 7. (a) Reversibility of PFOS and PFOA adsorption by addition of 50 vol.% methanol or
438 acetonitrile to the LDH particle suspension and (b) regeneration efficiency of spent CuMgFe-LDH
439 and PFOS/PFOA removal on reused CuMgFe-LDH. Experimental conditions: C_0 = 1.9 µmol/L for
440 PFOS or PFOA in Fig. 7a and 9.3 µmol/L in Fig. 7b, adsorbent dosages of 0.1 g/L in Fig. 7a and
441 0.5 g/L in Fig. 7b, and pH = 7.0. Error bars show deviations of single values from the mean of two
442 experiments.

443 **4 Conclusions**

444 Layered double hydroxide (LDH) with the metal composition of Cu(II)Mg(II)Fe(III) was prepared
445 as an adsorbent for fast adsorption of perfluorooctane sulfonate (PFOS) and perfluorooctanoate
446 (PFOA). In summary, the adsorption of PFOS and PFOA on CuMgFe-LDH occurs at high rates
447 with an equilibration time (≥95% of equilibrium loading) of about 1 h. The high adsorption rates
448 are facilitated by the small particle size of the LDH material (d_{50} = 3 µm). These particles are
449 obtainable by a simple bottom-up process. On the other hand, this particle size can be still separated
450 by sedimentation or micro-filtration from treated waters.

The adsorption was highly dependent on the PFAS chain lengths, indicating that hydrophobic interactions were the main driving force of PFAS adsorption. As a result, the adsorption affinity of PFOA on CuMgFe-LDH was lower than that of PFOS having K_d values up to 1×10^5 L/kg. The influence of ionic strength and pH value, combined with a strong competition effect by sulfate anions suggests that electrostatic attraction also plays a role in the adsorption which is more pronounced for PFOA than PFOS. However, no negative effects on PFOS and PFOA uptake were observed for monovalent inorganic anions with concentrations up to 10 mmol/L. Additionally, CuMgFe-LDO materials obtained after thermal treatment at 300℃ and 500℃ were considered poor in the adsorption of PFOS and PFOA and a previously reported 'memory effect' for uptake of these anions was not observed in the studied concentration range relevant for environmental media. The adsorbed fractions of PFOS and PFOA could be easily desorbed by solvent extraction using methanol or acetonitrile within 1 h. The regenerated CuMgFe-LDH maintained a good adsorption performance after two regeneration cycles.

Acknowledgements

This work was financially supported by International Cooperation and Exchange Program of Natural Science Foundation of China (Grant No. 41761134091), the Natural Science Foundation of Jiangsu Province (Grant No. BK20171519) and the China Scholarship Council.

References

[1] C.G. Pan, K.F. Yu, Y.H. Wang, W. Zhang, J. Zhang, J. Guo, Perfluoroalkyl substances in the riverine and coastal water of the Beibu Gulf, South China: Spatiotemporal distribution and source identification, Sci. Total Environ. 660 (2019) 297–305.

[2] J.P. Giesy, K. Kannan, Peer Reviewed: Perfluorochemical Surfactants in the Environment, Environ. Sci. Technol. 36 (2002) 146A-152A.

[3] Z. Du, S. Deng, Y. Bei, Q. Huang, B. Wang, J. Huang, G. Yu, Adsorption behavior and mechanism of perfluorinated compounds on various adsorbents-A review, J. Hazard. Mater. 274 (2014) 443–454.

[4] E.F. Houtz, C.P. Higgins, J.A. Field, D.L. Sedlak, Persistence of perfluoroalkyl acid precursors in AFFF-impacted groundwater and soil, Environ. Sci. Technol. 47 (2013) 8187–8195.

[5] L. Gobelius, J. Hedlund, W. Dürig, R. Tröger, K. Lilja, K. Wiberg, L. Ahrens, Per- and polyfluoroalkyl substances in swedish groundwater and Surface Water: Implications for environmental quality standards and drinking water guidelines, Environ. Sci. Technol. 52 (2018) 4340–4349.

[6] E.T. Chang, H.O. Adami, P. Boffetta, H.J. Wedner, J.S. Mandel, A critical review of perfluorooctanoate and perfluorooctanesulfonate exposure and immunological health conditions in humans, Crit. Rev. Toxicol. 46 (2016) 279–331.

[7] A. Karnjanapiboonwong, S.K. Deb, S. Subbiah, D. Wang, T.A. Anderson, Perfluoroalkylsulfonic and carboxylic acids in earthworms (Eisenia fetida): Accumulation and effects results from spiked soils at PFAS concentrations bracketing environmental relevance, Chemosphere. 199 (2018) 168–173.

[8] Z. Du, S. Deng, S. Zhang, W. Wang, B. Wang, J. Huang, Y. Wang, G. Yu, B. Xing, Selective and fast adsorption of perfluorooctanesulfonate from wastewater by magnetic fluorinated vermiculite, Environ. Sci. Technol. 51 (2017) 8027–8035.

[9] P.H. Chang, W.T. Jiang, Z. Li, Removal of perfluorooctanoic acid from water using calcined hydrotalcite – A mechanistic study, J. Hazard. Mater. 368 (2019) 487–495.

[10] H. Tian, C. Gu, Effects of different factors on photodefluorination of perfluorinated compounds by hydrated electrons in organo-montmorillonite system, Chemosphere. 191 (2018) 280–287.

[11] S. Wang, Q. Yang, F. Chen, J. Sun, K. Luo, F. Yao, X. Wang, D. Wang, X. Li, G. Zeng, Photocatalytic degradation of perfluorooctanoic acid and perfluorooctane sulfonate in water: A critical review, Chem. Eng. J. 328 (2017) 927–942.

[12] T.X.H. Le, H. Haflich, A. D. Shah, B. P. Chaplin, Energy-Efficient electrochemical oxidation of perfluoroalkyl substances using a Ti4O7 reactive electrochemical membrane anode, Environ. Sci. Technol. Lett. 6 (2019) 504–510.

[13] N. Saeidi, F.D. Kopinke, A. Georgi, Understanding the effect of carbon surface chemistry on adsorption of perfluorinated alkyl substances, Chem. Eng. J. 381 (2020) 122689.

[14] Q. Zhang, S. Deng, G. Yu, J. Huang, Removal of perfluorooctane sulfonate from aqueous solution by crosslinked chitosan beads: sorption kinetics and uptake mechanism, Bioresour. Technol. 102 (2011) 2265–2271.

[15] S. Deng, Q. Yu, J. Huang, G. Yu, Removal of perfluorooctane sulfonate from wastewater by anion exchange resins: Effects of resin properties and solution chemistry, Water Res. 44 (2010) 5188–5195.

[16] F. Cavani, F. Trifirò, A. Vaccari, Hydrotalcite-type anionic clays: Preparation, properties and applications., Catal. Today. 11 (1991) 173–301.

[17] C. Li, M. Wei, D.G. Evans, X. Duan, Layered double hydroxide-based nanomaterials as highly effi cient catalysts and adsorbents, Small. 10 (2014) 4469–4486.

[18] K.H. Goh, T.T. Lim, Z. Dong, Application of layered double hydroxides for removal of oxyanions: A review, Water Res. 42 (2008) 1343–1368.

[19] S.-H. Lee, M. Tanaka, Y. Takahashi, K.-W. Kim, Enhanced adsorption of arsenate and antimonate by calcined Mg/Al layered double hydroxide: Investigation of comparative adsorption mechanism by surface characterization, Chemosphere. 211 (2018) 903–911.

[20] T. Kameda, E. Kondo, T. Yoshioka, Preparation of Mg-Al layered double hydroxide doped with Fe^{2+} and its application to Cr(VI) removal, Sep. Purif. Technol. 122 (2014)

[21] P. Gu, S. Zhang, X. Li, X. Wang, T. Wen, R. Jehan, A. Alsaedi, T. Hayat, X. Wang, Recent advances in layered double hydroxide-based nanomaterials for the removal of radionuclides from aqueous solution, Environ. Pollut. 240 (2018) 493–505.

[22] P.C. Pavan, E.L. Crepaldi, J.B. Valim, Sorption of anionic surfactants on layered double hydroxides, J. Colloid Interface Sci. 229 (2000) 346–352.

[23] Z. Hu, X. Song, C. Wei, J. Liu, Behavior and mechanisms for sorptive removal of perfluorooctane sulfonate by layered double hydroxides, Chemosphere. 187 (2017) 196–205.

[24] Y. Chen, J. Yan, D. Ouyang, L. Qian, L. Han, M. Chen, Heterogeneously catalyzed persulfate by CuMgFe layered double oxide for the degradation of phenol, Appl. Catal. A Gen. 538 (2017) 19–26.

[25] D.Q. Zhang, W.L. Zhang, Y.N. Liang, Adsorption of perfluoroalkyl and polyfluoroalkyl substances (PFASs) from aqueous solution - A review, Sci. Total Environ. 694 (2019) 133606.

[26] F. Wang, C. Liu, K. Shih, Adsorption behavior of perfluorooctanesulfonate (PFOS) and perfluorooctanoate (PFOA) on boehmite, Chemosphere. 89 (2012) 1009–1014.

[27] H. Qiu, L. Lv, B. Pan, Q. Zhang, W. Zhang, Q. Zhang, Critical review in adsorption kinetic models, J. Zhejiang Univ. Sci. A. 10 (2009) 716–724.

[28] C. Yao, T. Chen, A new simplified method for estimating film mass transfer and surface diffusion coefficients from batch adsorption kinetic data, Chem. Eng. J. 265 (2015) 93–99.

[29] W. Chen, X. Zhang, M. Mamadiev, Z. Wang, Sorption of perfluorooctane sulfonate and perfluorooctanoate on polyacrylonitrile fiber-derived activated carbon fibers: In comparison with activated carbon, RSC Adv. 7 (2017) 927–938.

[30] F. Wang, K. Shih, Adsorption of perfluorooctanesulfonate (PFOS) and perfluorooctanoate (PFOA) on alumina: Influence of solution pH and cations, Water Res. 45 (2011) 2925–2930.

[31] K. Harada, F. Xu, K. Ono, T. Iijima, A. Koizumi, Effects of PFOS and PFOA on L-type Ca^{2+} currents in guinea-pig ventricular myocytes, Biochem. Biophys. Res. Commun. 329 (2005) 487–494.

[32] L. Yang, L. He, J. Xue, Y. Ma, Z. Xie, L. Wu, M. Huang, Z. Zhang, Persulfate-based degradation of perfluorooctanoic acid (PFOA) and perfluorooctane sulfonate (PFOS) in aqueous solution: Review on influences, mechanisms and prospective, J. Hazard. Mater. 393 (2020) 122405.

[33] C.Y. Tang, Q. Shiang Fu, D. Gao, C.S. Criddle, J.O. Leckie, Effect of solution chemistry on the adsorption of perfluorooctane sulfonate onto mineral surfaces, Water Res. 44 (2010) 2654–2662.

563 [34] F.L. Theiss, S.J. Couperthwaite, G.A. Ayoko, R.L. Frost, A review of the removal of
564 anions and oxyanions of the halogen elements from aqueous solution by layered double
565 hydroxides, J. Colloid Interface Sci. 417 (2014) 356–368.
566 [35] C.P. Higgins, R.G. Luthy, Sorption of perfluorinated surfactants on sediments, Environ.
567 Sci. Technol. 40 (2006) 7251–7256.
568 [36] E. Gagliano, M. Sgroi, P.P. Falciglia, F.G.A. Vagliasindi, P. Roccaro, Removal of poly-
569 and perfluoroalkyl substances (PFAS) from water by adsorption: Role of PFAS chain
570 length, effect of organic matter and challenges in adsorbent regeneration, Water Res. 171
571 (2020) 115381.
572 [37] B.D. Turner, S.W. Sloan, G.R. Currell, Novel remediation of per- and polyfluoroalkyl
573 substances (PFASs) from contaminated groundwater using Cannabis Sativa L. (hemp)
574 protein powder, Chemosphere. 229 (2019) 22–31.
575 [38] H. Chen, Y. Yao, Z. Zhao, Y. Wang, Q. Wang, C. Ren, B. Wang, H. Sun, A. C. Alder, K.
576 Kannan, Multimedia distribution and transfer of per- and polyfluoroalkyl substances
577 (PFASs) surrounding two fluorochemical manufacturing facilities in Fuxin, China,
578 Environ. Sci. Technol. 52 (2018) 8263–8271.
579 [39] Z.P. Xu, Y. Jin, S. Liu, Z.P. Hao, G.Q. (Max) Lu, Surface charging of layered double
580 hydroxides during dynamic interactions of anions at the interfaces, J. Colloid Interface Sci.
581 326 (2008) 522–529.
582 [40] Walter T. Reichle, Synthesis of anionic clay minerals (mixed metal hydroxides,
583 hydrotalcite), Solid State Ionics. 22 (1986) 135–141.
584 [41] R. Zhang, W. Yan, C. Jing, Mechanistic study of PFOS adsorption on kaolinite and
585 montmorillonite, Colloids Surfaces A Physicochem. Eng. Asp. 462 (2014) 252–258.
586
587